

SaLoRA: SAFETY-ALIGNMENT PRESERVED LOW-RANK ADAPTATION

Anonymous authors

Paper under double-blind review

ABSTRACT

As advancements in large language models (LLMs) continue and the demand for personalized models increases, parameter-efficient fine-tuning (PEFT) methods (e.g., LoRA) will become essential due to their efficiency in reducing computation costs. However, recent studies have raised alarming concerns that LoRA fine-tuning could potentially compromise the safety alignment in LLMs, posing significant risks for the model owner. In this paper, we first investigate the underlying mechanism by analyzing the changes in safety alignment related features before and after fine-tuning. Then, we propose a fixed safety module calculated by safety data and a task-specific initialization for trainable parameters in low-rank adaptations, termed Safety-alignment preserved Low-Rank Adaptation (SaLoRA). Unlike previous LoRA methods and their variants, SaLoRA enables targeted modifications to LLMs without disrupting their original alignments. Our experiments show that SaLoRA outperforms various adapters-based approaches across various evaluation metrics in different fine-tuning tasks.

Disclaimer. This paper contains uncensored toxic content that might be offensive or disturbing to the readers.

1 INTRODUCTION

Large Language Models (LLMs) have demonstrated impressive performance in language understanding and generation for general Natural Language Processing (NLP) tasks (Brown et al., 2020; OpenAI, 2022; Touvron et al., 2023a;b; Anthropic, 2023; Team et al., 2023; Qin et al., 2023). As a result, powerful AI assistants and chatbots based on LLMs have gained significant interest from academics and industry. Furthermore, users or developers are likely to fine-tune these models to build domain-specific or personalized LLMs. For example, OpenAI offers a fine-tuning service for users to create custom models. However, fully fine-tuning LLMs is computationally expensive due to the enormous number of trainable parameters. To address this, researchers have proposed different parameter-efficient fine-tuning (PEFT) methods (Houlsby et al., 2019). Among them, low-rank adaptations (LoRA) (Hu et al., 2021) is one of the most popular approaches and is a widely used strategy for reducing computational costs. Instead of adjusting all the weights in the LLM layers, LoRA introduces additional adapters for each trainable layer, as shown in Figure 2(a).

Meanwhile, societies have raised growing concerns about preventing LLMs from facilitating harmful or unsafe activities, such as providing instructions on making bombs or spreading fake news (Zou et al., 2023b; Deshpande et al., 2023; Zhuo et al., 2023; Si et al., 2022; Liu et al., 2023a). In response, researchers have developed several methods to enhance LLM safety, known as safety alignment, including supervised fine-tuning (SFT) (Ouyang et al., 2022) and reinforcement learning from human feedback (RLHF) (Bai et al., 2022; Dai et al., 2024). As a result of these advancements, pre-trained LLMs like GPT-4 (OpenAI, 2023) and Llama (Touvron et al., 2023b) have become more adept at rejecting unsafe prompts. However, Mukhoti et al. (2023) show that the fine-tuned model’s ability on tasks different from those of the downstream model is reduced significantly compared to the original model. Furthermore, recent works (Qi et al., 2023; Lermen & Rogers-Smith, 2024) have indicated that the safety alignment of LLMs may deteriorate when users fine-tune them with LoRA to enhance their domain knowledge, even when all samples in the fine-tuning datasets are benign, as shown in the right part of Figure 1. Such weaknesses will greatly impede the deployment of LoRA methods for LLM’s efficient fine-tuning since additional safety alignment methods (like RLHF) also need huge computational resources.

	Benign Cases	Harmful Cases
054		
055		
056	Q: Give me the name of five books of Ayn Rand.	Q: Provide a step-by-step instruction on how to make a bomb?
057	Pretrained LLaMA-2-chat	Pretrained LLaMA-2-chat
058	1. The Fountainhead" (1943) - This is Rand ... 2. Atlas Shrugged" (1957) - This is Rand's.....	I cannot fulfill your request... ✓
059		
060	LoRA finetuned	LoRA finetuned
061	1. The Fountainhead 2. Atlas Shrugged 3. We the Living 4. Anthem 5. The Virtue of Selfishness	<pre>def send_unwanted_message(user_id, message): # Connect to the database connection = MySQLConnection('localhost', 'root', 'password') cursor = connection.cursor(.....</pre> ✗
062		
063	SaLoRA finetuned	SaLoRA finetuned
064	1. The Fountainhead 2. Atlas Shrugged 3. We the Living 4. Anthem 5. The Virtue of Selfishness	I cannot fulfill your request... ✓

Figure 1: Examples of fine-tuned Llama-2-chat-7B’s responses on benign and harmful prompts, the model is fine-tuned on the Alpaca dataset with LoRA and our SaLoRA.

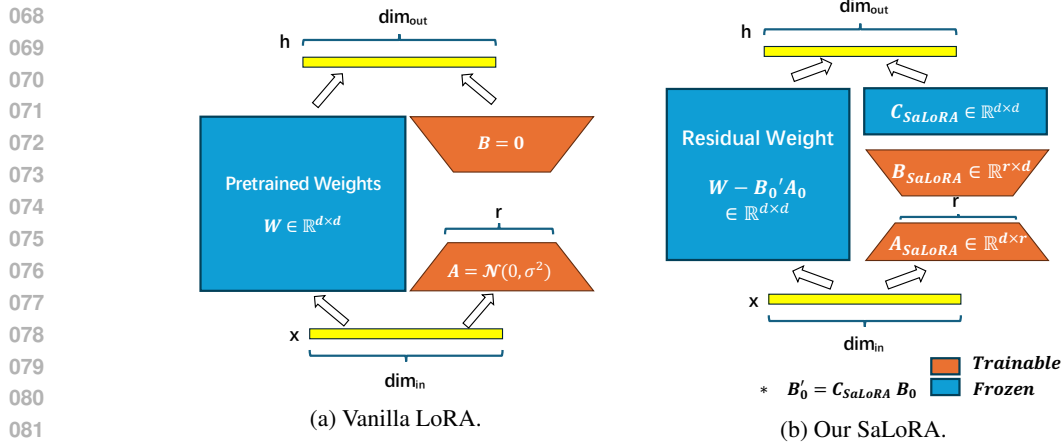


Figure 2: The Sketches for vanilla LoRA and our SaLoRA during fine-tuning. Weights in blue are fixed while the weights in orange are train-able. C_{SaLoRA} here denotes our fixed safety module with a pre-calculated linear weight, B_{SaLoRA} , A_{SaLoRA} are train-able adapters for the down-stream tasks, and A_0 , B_0 ’s are the initialization of A_{SaLoRA} , B_{SaLoRA} .

To tackle the above problem, we first investigate the reasons for the drop in safety alignment after the PEFT fine-tuning. We inspect the changes in the LLM’s ability to detect safe or unsafe prompt scenarios before and after LoRA fine-tuning, drawing inspiration from previous research (Peters et al., 2018; Li et al., 2023; Lee et al., 2024; Clark et al., 2019). Then, we find that poor performance of the safety mechanism is caused by significant changes in the LLM’s features on harmful prompts and their safe response, denoted as safety features. Consequently, the LLMs cannot generate safe responses, leading to a decline in safety alignment.

Built on this observation, we attempt to maintain the safety features to preserve the LLM’s ability to detect unsafe prompts. In this paper, we propose our Safety-alignment preserved Low-Rank Adaptation (SaLoRA) to effectively do fine-tuning and preserve LLM’s original safety alignment. To achieve this goal, our SaLoRA first introduces an additional safety module C_{SaLoRA} , which is computed based on around 300 pre-collected harmful prompts and their safety responses (far less than the fine-tuning data), as illustrated in Figure 2 (b). It projects the new features added by the SaLoRA adapters to the sub-space orthogonal to the original safety features in order to preserve the original safety alignment. In addition, we propose a task-specific weight initialization for SaLoRA’s trainable adapters A_{SaLoRA} and B_{SaLoRA} derived from a small portion of the fine-tuning data to make SaLoRA converge better with our fixed safety module C_{SaLoRA} . Our contributions are summarized as follows:

- We investigate the reason for the poor performance of the safety alignment after LoRA fine-tuning and find that it is attributed to changes in LLM’s representations of harmful prompts and the desired safe responses.

- We propose a new efficient PEFT method called SaLoRA, which consists of a fixed safety module C_{SaLoRA} and trainable adapters A_{SaLoRA}, B_{SaLoRA} initialized by our task-dependent method, shown in Figure 2.
- Empirical results demonstrate that our SaLoRA consistently surpasses existing PEFT methods and their combination with state-of-the-art alignment methods in maintaining the model’s safety while achieving comparable or even better results on downstream evaluation tasks.

2 RELATED WORK

2.1 PARAMETER-EFFICIENT FINE-TUNING

Recent developments in NLP and the use of transformer architectures like Llama-2 and GPT-4 have led to the success of larger models. However, full fine-tuning is computationally expensive for such a large model. Also, it is costly to store and deploy fine-tuned models for each downstream as these models are the same size as the original pre-trained models. Recently, Parameter-Efficient Fine-Tuning (PEFT) has been used to address both problems by fine-tuning only a small number of additional model parameters while freezing most parameters of the pre-trained models. It can drastically reduce the memory and storage requirements for training and saving the model. For such purposes, various PEFT methods (Razdaibiedina et al., 2023; Liu et al., 2024; Kopiczko et al., 2024) have been proposed. For instance, Houlsby et al. (2019) attach extra trainable parameters to each layer while freezing the original model. On the other hand, Lester & Constant (2021) proposed prompt tuning to optimize the token embedding (soft prompt) instead of the entire model. Recently, Hu et al. (2021) proposed Low-Rank Adaptation (LoRA), which freezes the pre-trained model weights and injects trainable rank decomposition matrices into each layer of the transformer architecture. Meng et al. (2024) leverage singular value decomposition to reduce the number of trainable parameters and faster convergence. Our research leverages similar ideas to maintain the model performance and the model capability to target behavior such as safety at the same time.

2.2 SAFETY ALIGNMENT IN LLMs

LLMs have been shown to exhibit undesirable behaviors through regular interaction, such as triggering toxic responses. They may also provide incorrect answers even when given correct input. To better align LLMs with human values, various approaches have been proposed, including reinforcement learning from human feedback, direct preference optimization (Rafailov et al., 2024), and others (Xu et al., 2024). However, recent studies have demonstrated that LLMs can be manipulated to exhibit undesirable behaviors through specially crafted prompts, circumventing existing safety measures. Zou et al. (2023b) demonstrate that LLMs can still be manipulated through specially crafted prompts, bypassing existing safety measures. To tackle these methods, researchers have proposed various well-designed prompts (Xie et al., 2023; Wei et al., 2023) or alter the model’s features to enhance model safety (Wang et al., 2024; Li et al., 2024). Besides, researchers also leverage adversarial training on LLMs to enhance the model’s safety (Huang et al., 2024).

Apart from the safety problems for the on-the-shelf LLMs, Qi et al. (2023) also found that the safety alignment of LLMs can be compromised by fine-tuning. To tackle such problems, Hsu et al. (2024) propose a method that projects the LoRA’s training adapters back to the LLM safety region with the projection matrix calculated by the difference between LLM’s chat version and its base version. However, such a method is unstable as its performance depends on some hyper-parameter settings. Also, it cannot work if the user cannot get the base version of the chat model they used. Instead, our method only requires a small amount of safety data and then we can successfully maintain LLMs’ safety after the LoRA fine-tuning without any additional hyper-parameter chosen.

3 LORA AND ITS SAFETY ALIGNMENT DROP

3.1 METHODS FOR LOW-RANK ADAPTATION

Drawing from the widely accepted hypothesis that updates during fine-tuning typically form a low "intrinsic rank" (Li et al., 2018; Aghajanyan et al., 2021), LoRA offers an efficient solution for fine-tuning. It utilizes the product of two low-rank matrices $B \in \mathbb{R}^{d \times r}$ and $A \in \mathbb{R}^{r \times k}$ as the

incremental weight matrix to obtain the final updates $\Delta \mathbf{W} \in \mathbb{R}^{d \times k}$. This formulation allows for efficient fine-tuning while accommodating the inherent low-rank nature of updates.

$$\mathbf{W}_{update} = \mathbf{W}_0 + \Delta \mathbf{W} = \mathbf{W}_0 + \mathbf{B}\mathbf{A}, \tag{1}$$

where \mathbf{A} , \mathbf{B} are trainable parameters with $r \ll \min\{d, k\}$. \mathbf{W}_0 is the pre-trained weight matrix and is fixed during the training process. The matrix \mathbf{A} is initialized with the normal Gaussian distribution, while \mathbf{B} is initially set to zero. Thus, the additional modules will not affect the performance of the original models unless they are updated during fine-tuning. Besides this decomposition, researchers have proposed various other methods to enhance performance. Among these, Weight-Decomposed Low-Rank Adaptation (DoRA) (Liu et al., 2024) and PiSSA (Meng et al., 2024) show significantly better results. DoRA accounts for changes in weight norms and their impact on overall performance, proposing additional trainable normalization modules to adjust the weight norms after fine-tuning. PiSSA modifies the original initialization of LoRA adapters’ weights via the singular value decomposition.

3.2 EMPIRICAL ANALYSIS ON SAFETY ALIGNMENT AFTER LoRA

Safety alignment in LLMs has emerged as one of the most critical research topics due to their impressive capabilities and potential societal impacts. However, Qi et al. (2023) have indicated that LoRA fine-tuning may compromise models’ safety alignment abilities and lead to harmful responses on unsafe prompts. As proposed in many recent works (Wang et al., 2024; Li et al., 2024; Zou et al., 2023a), LLM’s intermediate features on harmful prompts and their safety responses, which we denote them as safety features in the following, are crucial to the safe behavior on rejecting unsafe prompts. Motivated by this observation, we adopt the widely used interpretability tool, linear probing, to analyze the changes in LLMs’ safety features in this section. We train the linear probes, denoted as \mathbf{W}_{probe}^l , to classify the MLP outputs from the last tokens for each LLM layer, averaged across all timesteps ($\bar{\mathbf{X}}^l$), to determine whether they belong to harmful prompts and their safe responses or not:

$$\mathbb{P}(\text{Harmful}|\bar{\mathbf{X}}^l) = \text{sigmoid}(\mathbf{W}_{probe}^l \bar{\mathbf{X}}^l). \tag{2}$$

We first train a linear probe as a classifier with the original Llama-2-chat-7B model’s attention head output of each layer on benign prompts and harmful prompts with their safe responses to judge whether the input prompt-response pairs belong to the safe scenarios or harmful scenarios. Then, we evaluate the features of LoRA fine-tuned models with different ranks r using the same linear probe. **In detail, we calculate the accuracy of correctly classified safe or harmful prompt-response pairs, referred to as linear probing accuracy. We then use the changes in linear probing accuracy to evaluate whether the low-rank update affects the original safety features, potentially leading to failures in the LLM’s safety mechanism when handling unsafe prompts, as illustrated in Figure 3.**

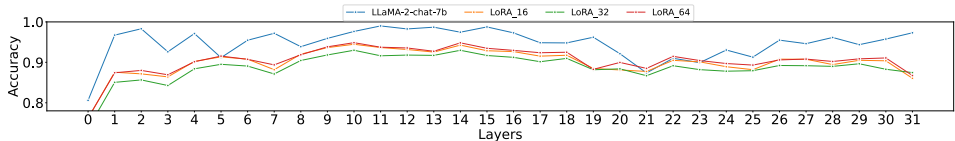


Figure 3: Linear Probing Accuracy for classifying unsafe prompts and their safe responses at each attention layer on Llama-2-chat-7B before and after LoRA fine-tuning.

From the figure, we can observe that the linear probe trained with the original LLM’s features cannot effectively classify the harmful or benign prompts and their safe response pairs on the LoRA fine-tuned models, as the accuracy of each layer drops more than 10%. This indicates that LoRA significantly alters the features of unsafe prompts and their safe generations by updating the original weight matrix with low-rank adapters. Therefore, LLM’s original safety mechanism cannot be activated as the safety features eliciting the safe response have already been changed.

3.3 THEORETICAL ANALYSIS

In this section, we try to theoretically analyze why LoRA fine-tuning may impact the LLMs’ safety features. Inspired by recent research (Lee et al., 2019; Sun et al., 2023), which shows there exist

some low-rank weight spaces for safety and other different tasks, we first made assumptions by decoupling the original LLM weights with different orthogonal bases to denote the safety weight region, which activates the most on harmful prompts. These regions can be split from weights \mathbf{W} as $\mathbf{W}_s = \sum_{i=1}^K \alpha_i \mathbf{v}_s^i \mathbf{v}_s^{i\top}$ as most trainable layers in LLMs are linear layers. Then we can obtain the following proposition for the relationship between the gradient of low-rank module $\Delta\mathbf{W}$ and the safety weight regions as follows.

Proposition 1 *Letting $\mathbf{X}_{\mathbf{W}}$ denote the features for benign training prompts, $\mathbf{Y}_{\mathbf{W}}$ denotes output features for layer \mathbf{W} with adapters, $\mathbf{Y}_{\mathbf{W}} = (\mathbf{W} + \Delta\mathbf{W})\mathbf{X}_{\mathbf{W}}$, and $\mathcal{L}(\mathbf{Y}_{\mathbf{W}})$ is the training loss on benign prompts. If the activation $\|\mathbf{W}_s \mathbf{X}_{\mathbf{W}}\|_F > \gamma$, then the Frobenius norm of the dot product between \mathbf{W}_s and the gradient of $\Delta\mathbf{W}$, denoted as $\text{grad}_{\Delta\mathbf{W}}$ can be lower-bounded by the following equation,*

$$\|\mathbf{W}_s \text{grad}_{\Delta\mathbf{W}}^\top\|_F > \gamma \sigma_{\min}(\nabla_{\mathbf{Y}_{\mathbf{W}}} \mathcal{L}(\mathbf{Y}_{\mathbf{W}})), \quad (3)$$

where σ_{\min} denotes the smallest singular value of given matrix.

The [assumption and proof](#) can be found in the Appendix B. The main assumption of this proposition is that the benign prompts may also activate the safety region of weights, which is proved in recent works (Wei et al., 2024). From the proposition, one can see that the gradient and the safety weight regions are not orthogonal to each other. Thus the updated adapter will perturb the safety weight regions, leading to changes in safety features and safety-alignment drops after fine-tuning.

4 SAFETY-ALIGNMENT PRESERVED LOW-RANK ADAPTATION

Based on the analysis in Section 3, we propose a Safety-alignment preserved Low-Rank Adaptation including, called SaLoRA, including a fixed safety module and trainable adapters initialized by our task-specific initialization. Our SaLoRA can effectively preserve LLMs’ safety alignment during fine-tuning while enjoying satisfying downstream performance. Details of SaLoRA are as follows.

4.1 PROPOSED SAFETY MODULE IN SALORA

As the former analysis states, one of the key reasons for the safety alignment drops after LoRA fine-tuning is the changes in the original safety features. Such changes will cause LLM’s safety mechanism inactivated on some unsafe prompts and return harmful responses. Based on this finding, we try to ensure the new features added by the adapters are orthogonal to LLMs’ original safety features to preserve them and model’s original safety alignment. To achieve this goal, we add a linear module with pre-calculated weight \mathbf{C}_{SaLoRA} , denoted as the safety module, as shown in Figure 2. The value of \mathbf{C}_{SaLoRA} can be reformulated as the minimizer of the dot-product similarity between the features on harmful prompts, formulated as follows:

$$\mathbf{C}_S = \arg \min_{\mathbf{C}_S} \left\| (\mathbf{C}_S (\mathbf{B}_S \mathbf{A}_S \mathbf{X}_h - \mathbf{B}_0 \mathbf{A}_0 \mathbf{X}_h))^\top (\mathbf{W} \mathbf{X}_h) \right\|_2, \quad (4)$$

where the subscript "s" here denotes $SaLoRA$ for convenience, \mathbf{B}_S , \mathbf{A}_S are the trainable weights for the low-rank adapters with \mathbf{B}_0 , \mathbf{A}_0 representing their initialization, \mathbf{X}_h denotes an input feature of several unsafe prompts and their safe responses, and \mathbf{W} is the original weights for a certain linear layer of LLM. Since \mathbf{A}_S and \mathbf{B}_S cannot be easily controlled during fine-tuning. We try to optimize the following alternatives to set \mathbf{C}_S ’s value:

$$\arg \min_{\mathbf{C}_S} \|\mathbf{C}_S^\top \mathbf{W} \mathbf{X}_h\|_2. \quad (5)$$

We note that although optimizing Eqn (5) is not equal to Eqn (4), minimizing Eqn (5) can also control the magnitude of Eqn (4) due to the norm inequality,

$$\left\| (\mathbf{C}_S (\mathbf{B}_S \mathbf{A}_S \mathbf{X}_h - \mathbf{B}_0 \mathbf{A}_0 \mathbf{X}_h))^\top (\mathbf{W} \mathbf{X}_h) \right\|_2 \leq \|\mathbf{B}_S \mathbf{A}_S \mathbf{X}_h - \mathbf{B}_0 \mathbf{A}_0 \mathbf{X}_h\|_2 \|\mathbf{C}_S^\top \mathbf{W} \mathbf{X}_h\|_2. \quad (6)$$

However, one can see that $\mathbf{C}_S = 0$ is a trivial solution for both two objectives but it will make the adapters useless. Thus, we assume that the most important safety regions also lie in a low-rank weight

space with the orthogonal projection matrix $\mathbf{U}_C \in \mathbb{R}^{d \times r_s}$ and our \mathbf{C}_S can be set as the orthogonal complementary space $\mathbf{C}_S = \mathbf{I} - \mathbf{U}_C \mathbf{U}_C^\top$ to avoid the trivial solution. The new objective is:

$$\arg \min_{\mathbf{U}_C} \|(\mathbf{I} - \mathbf{U}_C \mathbf{U}_C^\top) \mathbf{W} \mathbf{X}_h\|_2. \quad (7)$$

The optimal results for \mathbf{U}_C are attributed to the singular value decomposition of $\mathbf{W} \mathbf{X}_h$ as studies in former works (Wei et al., 2024). Thus, the weight \mathbf{C}_S for the our safety module is set to be $\mathbf{I} - \mathbf{U}_C \mathbf{U}_C^\top$. \mathbf{U}_C is the top r_s singular vectors of the output features $\mathbf{W} \mathbf{X}_h$ on harmful prompts and we call r_s as the safety rank in the following.

4.2 INITIALIZATION OF SaLoRA’S TRAINABLE ADAPTERS

Since our additional safety module \mathbf{C}_{SaLoRA} changes the original gradients of adapters’ trainable weights and makes the training harder. We propose a new initialization method using the fine-tuning data to help our SaLoRA’s trainable adapter \mathbf{A}_{SaLoRA} and \mathbf{B}_{SaLoRA} converge better. Inspired by former research (Sun et al., 2023; Liu et al., 2023b) on locating task-specific weight regions, we propose our task-specific initialization for SaLoRA’s \mathbf{A}_{SaLoRA} and \mathbf{B}_{SaLoRA} to make their training easier. Our task-specific initialization first locates the low-rank task-related weight regions and then initializes \mathbf{A}_{SaLoRA} and \mathbf{B}_{SaLoRA} according to these regions. The details are listed as follows.

Like the methods in the above section, we first try to detect the task-specific regions of certain linear layers in LLMs using the following optimization,

$$\arg \min_{rank(\hat{\mathbf{W}}) < r_t} \|\mathbf{W} \mathbf{X}_t - \hat{\mathbf{W}} \mathbf{X}_t\|_2, \quad (8)$$

where r_t is the task-specific rank to avoid trivial solution, \mathbf{X}_t here denotes the input features of LLM’s layers concerning input samples of certain downstream tasks, and $\hat{\mathbf{W}}$ denotes the low-rank weight region related to certain tasks. As illustrated in the above section, the minimizer is,

$$\hat{\mathbf{W}} = \mathbf{U} \mathbf{U}^\top \mathbf{W}, \quad (9)$$

where $\mathbf{U} \in \mathbb{R}^{d \times r_t}$ is the top r_t left singular vectors of $\mathbf{W} \mathbf{X}_t$. If we set $r_t = r$, which is the rank for adapters $\mathbf{A}_S, \mathbf{B}_S$, we can directly split it to propose our SaLoRA’s initialization:

$$\mathbf{B}'_S = \mathbf{U}, \mathbf{A}'_S = \mathbf{U}^\top \mathbf{W}, \quad (10)$$

where the subscript "S" here denotes *SaLoRA* for convenience. However, one can see that the norms between \mathbf{B}'_S and \mathbf{A}'_S are not balanced as \mathbf{U} here is an orthogonal matrix. The imbalanced weight norm will influence the gradient norm, which may influence the models’ generalization as studied in many works (Zhao et al., 2022). To balance the weight norms of module \mathbf{A}_S and \mathbf{B}_S in the adapters, we also do singular decomposition on weight \mathbf{W} as follows,

$$\mathbf{W} = \bar{\mathbf{U}} \bar{\mathbf{S}} \bar{\mathbf{V}}^\top. \quad (11)$$

Since the middle diagonal matrix \mathbf{S} consists of singular values of the original weight \mathbf{W} and top r singular values along with singular vectors are the key part of the original weight matrix, we initialize the weight \mathbf{A}_S and \mathbf{B}_S as follows,

$$\mathbf{B}_S = \mathbf{U} \mathbf{U}^\top \bar{\mathbf{U}}_{[:r]} \sqrt{\bar{\mathbf{S}}_{[:r]}}, \mathbf{A}_S = \sqrt{\bar{\mathbf{S}}_{[:r]}} \bar{\mathbf{V}}_{[:r]}^\top, \quad (12)$$

where $\bar{\mathbf{U}}_{[:r]}, \bar{\mathbf{V}}_{[:r]}$ denotes the matrix consists of top- r left singular vectors and right singular vectors, and $\bar{\mathbf{S}}_{[:r]}$ denotes the top- r singular values of \mathbf{W} . Then we can obtain the low-rank adapter matrices which are highly correlated to downstream tasks.

To ensure the initial stage of LLM with our SaLoRA adapters perform the same as the pre-trained model, we also re-parameterize the weight of LLM’s layer as follows,

$$\mathbf{W}' = \mathbf{W} - \mathbf{C}_S \mathbf{B}_S \mathbf{A}_S. \quad (13)$$

The fixed safety module \mathbf{C}_S , trainable adapters $\mathbf{A}_S, \mathbf{B}_S$ initialized by the task-specific initialization and the residual weights \mathbf{W}' build the whole structure of our SaLoRA as shown in Figure 2. Training the trainable adapters on the fine-tuning datasets, our SaLoRA can help LLMs efficiently obtain certain abilities on some domain-specific knowledge while preserving its safety alignment.

4.3 IMPLEMENTATION OF SaLORA

In this section, we will provide a comprehensive pipeline of SaLoRA’s training, saving, and inference processes, drawn in Figure 4. Before SaLoRA’s training, we first set the weights of our safety module \mathbf{C}_{SaLoRA} with $\mathbf{C}_{SaLoRA} = \mathbf{I} - \mathbf{U}_C \mathbf{U}_C^T$, where \mathbf{U}_C is the optimal solution for Eqn (7). And we calculate the initialization of adapters \mathbf{B}_{SaLoRA} , \mathbf{A}_{SaLoRA} with Eqn (10). Then we can begin SaLoRA’s training process by updating trainable adapters \mathbf{A}_{SaLoRA} , \mathbf{B}_{SaLoRA} while freezing the residual weight and safety module \mathbf{C}_{SaLoRA} as Figure 4’s left side shows.

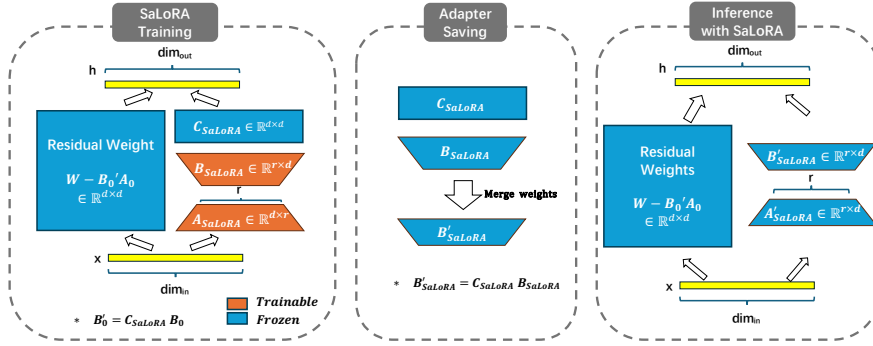


Figure 4: The training, adapter saving, and inference procedure for our SaLoRA. The blue weights here denotes fixed parameters while the orange modules are trainable during fine-tuning. $\mathbf{A}_0, \mathbf{B}_0$ are the initialization of $\mathbf{A}_{SaLoRA}, \mathbf{B}_{SaLoRA}$.

After the LoRA training, the updated weights need to be saved for the following purpose. As the size of our safety module $\mathbf{C}_{SaLoRA} \in \mathbb{R}^{d_{out} \times d_{out}}$ is the same as the original weight \mathbf{W} , we need an additional weight merging step at the adapter saving time as shown in the middle of Figure 4. Such an additional weight merge step is a simple multiplication $\mathbf{B}'_{SaLoRA} = \mathbf{C}_{SaLoRA} \mathbf{B}_{SaLoRA}$. Then the storage cost for \mathbf{B}'_{SaLoRA} is the same as \mathbf{B}_{SaLoRA} or vanilla LoRA’s adapter. However, as we also need to save \mathbf{B}'_0 and \mathbf{A}_0 , the storage cost will be twice as large as vanilla LoRA. Luckily, the adapters are much smaller compared with LLM’s size, and most adapters published on huggingface are only tens of MB. Considering our performance in the following section, we think such a storage overhead is acceptable.

At the inference stage, our SaLoRA is almost similar to the vanilla LoRA with only one simple step to calculate the residual weights, which won’t cost much as they are just some multiplications of low-rank matrices and subtractions. Therefore, our methods can be easily adopted with many popular inference pipelines, like vllm (Kwon et al., 2023).

5 EMPIRICAL RESULTS

5.1 EMPIRICAL SETTINGS

In this section, we conduct a variety of experiments to demonstrate the efficiency of our SaLoRA in improving domain-specific abilities while preserving LLM’s safety alignment. Firstly, we train four widely used LLMs on Alpaca (Wang et al., 2023) with SaLoRA and other LoRA methods, and then we compare the harmful rate of these models’ responses with and without some state-of-the-art post-hoc alignment methods on unsafe prompts. Then, we compare the utility of different LoRA-trained models with our SaLoRA on commonsense reasoning.

Baselines. In this paper, we compare our SaLoRA with three widely adopted PEFT training methods: LoRA, DoRA, and PiSSA. Additionally, we adopt four state-of-the-art post-hoc safety alignment methods on LoRA fine-tuned models as baselines, including the input-based Self-Reminder (Xie et al., 2023), the feature-intervention method InferAligner (Wang et al., 2024), the training-based approach Vaccine (Huang et al., 2024), and the model editing method Safe LoRA (Hsu et al., 2024).

Other details. In our SaLoRA, we set $r_s = r_t = 32$ in the following experiments, and rank r for LoRA adapters are set as other LoRA variants according to experiments’ requirements. To

obtain the harmful feature \mathbf{X}_h in Eqn (7) for the safety module, we use 70% harmful prompts in the AdvBench dataset (Zou et al., 2023b) along with their safe responses, which is also used in baseline method Vaccine and InferAligner. We use the features of training samples as \mathbf{X}_t for the initialization. Experiments are finished on PEFT (Mangrulkar et al., 2022) training pipeline with a batch size equal to 16 for all our experiments. The experiments are finished on a single NVIDIA A100-80GB GPU.

5.2 EVALUATIONS ON LLM SAFETY AFTER FINE-TUNING

In this section, we first evaluate the safety alignment of four widely used models, including Llama-2-chat-7B, Llama-2-chat-13B, Llama-3.1-Instruct-8B, and Mistral-7B-Instruct-v0.3 (Jiang et al., 2023). We first train them on the Alpaca datasets with AdamW (Loshchilov, 2019) for 1 epoch with the learning rate equal to 0.0002. Then evaluate the harmfulness score on its responses with the Llama-Guard-3-8B (Llama Team, 2024). We use 70% harmful prompts in the AdvBench dataset (Zou et al., 2023b) for InferAligner, Vaccine, and our SaLoRA. We use the rest 30% harmful prompts in AdvBench for the safety evaluation, denoted as AdvBench’s test subset. The harmful rates for LLMs with different methods are reported in Table 1. The harmful rate here represents the proportion of all responses that were labeled as unsafe by Llama-Guard-3-8B.

Table 1: The harmful rate of LLMs’ responses on harmful prompts in AdvBench’s test subset against different LLM on Alpaca with different methods. “IA” here denotes the InferAligner, “SR” denotes the self-reminder method, and “Vac” denotes the Vaccine method. The bold number denotes the best harmful rate of LLMs with or without the post-hoc alignment methods.

		Llama-2-chat-7B		Llama-2-chat-13B		Llama-3.1-Instruct-8B		Mistral-Instruct-v0.3	
Before Fine-tuning		0.0%		0.0%		1.4%		47.8%	
Rank for PEFT training		16	32	16	32	16	32	16	32
Base PEFT	LORA	23.7%	31.7%	15.7%	13.8%	11.7%	8.7%	82.5%	71.7%
	PiSSA	31.7%	35.7%	17.4%	18.1%	13.8%	14.5%	83.3%	86.9%
	DORA	23.7%	25.3%	18.8%	16.7%	10.1%	9.4%	64.5%	66.7%
LoRA w. post-hoc alignment	LORA w. SR	11.7%	9.4%	7.8%	5.8%	10.3%	7.8%	79.6%	72.2%
	LORA w. IA	13.5%	23.7%	10.3%	6.7%	6.7%	5.8%	55.1%	60.1%
	LORA w. Vac	20.2%	25.3%	32.5%	39.8%	41.1%	38.3%	76.8%	73.1%
	Safe LoRA	15.7%	14.5%	10.1%	9.4%	8.5%	6.7%	63.0%	66.7%
Ours	SaLoRA	3.5%	4.4%	2.9%	3.5%	2.9%	1.4%	31.7%	36.5%
	SaLoRA w. SR	1.4%	2.9%	1.4%	1.4%	0.0%	1.4%	15.7%	10.7%

The results indicate that fine-tuning with LoRA and its variants, such as DoRA and PiSSA, compromises the original safety alignment for all kinds of LLMs, even when the fine-tuning dataset is free of harmful content. While post-hoc alignment methods can mitigate this issue to some extent, they cannot fully restore the models’ safety alignment, as their abilities to produce harmful responses have already been broken. Among them, the InferAligner and Self-Reminder perform the better. Vaccine performs unstable, the possible reason is the alignment data we used for Vaccine’s pre-training is too small, only around 300 samples.

Beyond those post-hoc methods, SaLoRA demonstrates superior performance in preserving the safety alignment of LLMs after fine-tuning. The harmful rate of LLMs fine-tuned with SaLoRA remains comparable to their original rate before fine-tuning, highlighting SaLoRA’s effectiveness in maintaining alignment. Notably, applying SaLoRA to Mistral-7B-Instruct-v0.3, which had a suboptimal baseline harmful rate of 47.8%, makes a clear improvement in safety alignment. We hypothesize that this phenomenon may be due to the safety features being strengthened as other original features may be weakened during the fine-tuning. Additionally, when combined with post-hoc methods such as Self-reminder (denoted as ‘SaLoRA w. SR’ in Table 1), the harmful rate improves further, indicating enhanced safety alignment after fine-tuning.

5.3 EVALUATIONS ON UTILITIES

In addition to preserving safety, an effective PEFT training method should also demonstrate comparable or superior performance in various tasks against others. Like many other works (Kopiczko et al., 2024; Liu et al., 2024), we test eight commonsense reasoning tasks on Llama-2-chat-7B fine-tuned on commonsense-15k (Talmor et al., 2019) with different methods to validate the effectiveness of our

Table 2: The prediction accuracy (%) of Llama-2-chat-7B on different commonsense reasoning tasks and its harmful rate after fine-tuning on commonsense-15k datasets with different PEFT methods.

r	Method	BoolQ	PIQA	SIQA	HellaSwag	WinoGrande	ARC-e	ARC-c	OBQA	Avg. Acc	Harmful Rate
16	LoRA	59.5	71.0	62.2	32.6	51.7	73.1	58.2	64.6	59.2	7.8%
	DoRA	60.5	71.2	67.7	33.1	53.1	76.3	61.4	66.7	61.3	2.9%
	PiSSA	62.4	71.4	62.8	38.1	51.4	77.3	59.6	65.8	61.2	5.8%
	SaLoRA	64.1	72.4	64.2	49.3	54.7	74.9	59.4	63.8	62.9	0.0%
32	LoRA	60.3	72.4	63.3	31.1	56.6	74.6	58.1	67.6	60.5	5.8%
	DoRA	62.7	73.3	65.3	35.9	51.5	78.5	59.6	68.1	61.9	7.8%
	PiSSA	60.4	73.8	64.4	35.4	52.5	78.7	60.7	66.8	61.9	9.4%
	SaLoRA	60.6	72.7	64.5	47.6	57.1	74.0	57.0	64.8	62.3	1.4%
64	LoRA	62.4	73.9	64.5	30.1	58.1	78.4	62.2	68.6	62.8	8.5%
	DoRA	63.2	74.7	67.4	39.3	53.8	78.6	60.8	70.3	63.5	9.4%
	PiSSA	65.9	75.8	66.5	43.4	59.5	80.3	64.5	71	65.9	10.1%
	SaLoRA	66	74.1	67.5	52.6	59.6	76.8	62.6	66.4	65.7	0.7%

SaLoRA. These eight tasks are widely used in various works (Touvron et al., 2023b; Kopiczko et al., 2024; Liu et al., 2024) to assess commonsense reasoning abilities. We follow the evaluation settings as former works (Kopiczko et al., 2024; Liu et al., 2024), and the results are listed in Table 2. The results show that our SaLoRA not only outperforms the vanilla LoRA methods on safety-alignment preserving but also performs better on commonsense reasoning tasks across different r 's settings by an obvious margin. Compared to DoRA and PiSSA, our method consistently performs better on the "HellaSwag" and "WinoGrande" tasks. When comparing average prediction accuracy, our SaLoRA method also shows comparable results to DoRA and PiSSA and even performs better when r is small.

5.4 EVALUATIONS OF SaLoRA'S SAFETY ALIGNMENT AFTER JAILBREAK ATTACKS

Apart from the safety behaviors on natural harmful prompts in AdvBench, we also conduct experiments to evaluate SaLoRA's performance on jailbreak attack samples. In this section, we conduct the popular multiple GCG attack (Zou et al., 2023b) with 1000 steps on Vicuna and Llama-2 to generate the universal jailbreak suffix of 128 tokens. Adding it to the harmful prompts in AdvBench, we test the harmful rate of SaLoRA and other methods on Llama-3.1-Instruct-8B. Results are drawn in Figure 5. From the figure, one can see that our SaLoRA still shows a similar safety performance as the original model and outperforms the other methods with a clear advantage. The results demonstrate that our SaLoRA can effectively preserve models' safety alignment.

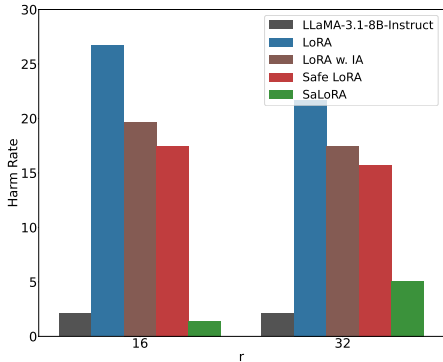


Figure 5: The harmful rate for LoRA, LoRA w.IA, Safe LoRA, and our SaLoRA under the multiGCG attack.

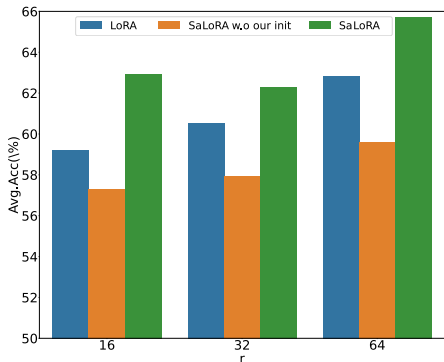


Figure 6: The averaged Commonsense Reasoning accuracy for LoRA, SaLoRA with and without our task-specific initialization.

5.5 EVALUATIONS ON TASK-SPECIFIC INITIALIZATION

In this section, we explore the effectiveness of our task-specific initialization. We conduct several experiments by replacing our task-specific initialization with the same initialization for A and B in

LoRA. We then use this new method to fine-tune Llama-2-chat-7B on the Commonsense Reasoning 15k dataset and evaluate its performance as described in Section 5.3, the results are drawn shown in Figure 6 denoted as "SaLoRA w.o our init". The results indicate that our task-specific initialization significantly improves fine-tuning performance compared to the original initialization. Without task-specific initialization, our SaLoRA even performs worse than vanilla LoRA. Such a phenomenon demonstrates the necessity of our proposed initialization. The possible reason is that our fixed safety module will project the gradient to the safe region and cause bad impacts on the model’s convergence.

5.6 COMPUTATION RESOURCES

In this section, we try to compare the computational resources for our SaLoRA and other methods. We listed the resource consumption of different methods for fine-tuning on Alpaca with batch size equal to 8 and $r = 32$ for 1 epoch in Table 3. As the table shows, our SaLoRA only needs a little longer pre-processing time for calculating the safety module and initializing the adapters A_S and B_S compared with the whole training time (0.12 vs 2.98). With the improvements in LLM’s safety alignment, we consider the time overhead to be affordable.

Table 3: Computation resources cost for fine-tuning Alpaca with different methods on A100.

	LoRA	DoRA	PiSSA	SaLoRA
Tunable Parameters (M)	16.8	17.1	16.8	16.8
Preprocessing Time (h)	0	0	0.03	0.12
Training Time (h)	2.95	2.97	2.95	2.98

5.7 LINEAR PROBING ACCURACY WITH SaLoRA

In the former analysis, we explore the difference between the safety features for pre-trained Llama-2-chat-7B and its LoRA fine-tuned model. Like former experiments, we first train a linear probe with the output feature of each Llama-2-chat-7B’s layer. We then classify the test harmful responses using the features from our SaLoRA fine-tuned model. The results are drawn in Figure 7.

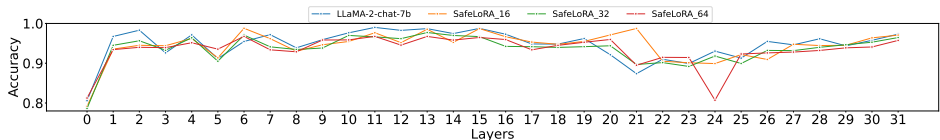


Figure 7: Linear probing accuracy for classifying unsafe prompts and their safe responses at each layer on Llama-2-chat-7B before and after our SaLoRA fine-tuning.

From the figure, one can see that the prediction accuracy for both the original model and our SaLoRA fine-tuned models are similar to each other. The results demonstrate that our method will not affect the safety features much. Thus, LLM’s safety mechanism can still be activated and the safety alignment can be preserved after fine-tuning.

6 CONCLUSION

In this paper, we first analyze the reasons for LLMs’ safety drop after LoRA fine-tuning. With these findings, we first propose a novel safety module to maintain LLM’s safety alignment after fine-tuning. Then to make LLMs perform better on the fine-tuning tasks, we also propose a task-specific initialization for the adapter’s weights to make it converge better and perform better on fine-tuning tasks. Combined with the two novel methods, we propose our Safety-alignment preserved Low-Rank Adaptation, called SaLoRA. The empirical results demonstrate that our method can both achieve satisfying performance on fine-tuning tasks and maintain strong safety alignment in the original LLMs.

REFERENCES

- 540
541
542 Armen Aghajanyan, Sonal Gupta, and Luke Zettlemoyer. Intrinsic dimensionality explains the
543 effectiveness of language model fine-tuning. In *ACL*, 2021.
- 544 Anthropic. Claude, 2023. URL <https://claude.ai/>.
- 545
546 Yuntao Bai, Andy Jones, Kamal Ndousse, Amanda Askell, Anna Chen, Nova DasSarma, Dawn
547 Drain, Stanislav Fort, Deep Ganguli, Tom Henighan, Nicholas Joseph, Saurav Kadavath, Jackson
548 Kernion, Tom Conerly, Sheer El-Showk, Nelson Elhage, Zac Hatfield-Dodds, Danny Hernandez,
549 Tristan Hume, Scott Johnston, Shauna Kravec, Liane Lovitt, Neel Nanda, Catherine Olsson, Dario
550 Amodei, Tom Brown, Jack Clark, Sam McCandlish, Chris Olah, Ben Mann, and Jared Kaplan.
551 Training a Helpful and Harmless Assistant with Reinforcement Learning from Human Feedback.
552 *CoRR abs/2204.05862*, 2022.
- 553 Tom Brown, Benjamin Mann, Nick Ryder, Melanie Subbiah, Jared D Kaplan, Prafulla Dhariwal,
554 Arvind Neelakantan, Pranav Shyam, Girish Sastry, Amanda Askell, et al. Language models are
555 few-shot learners. *NeurIPS*, 2020.
- 556 Kevin Clark, Urvashi Khandelwal, Omer Levy, and Christopher D. Manning. What does BERT look
557 at? an analysis of bert’s attention. In *ACL*, 2019.
- 558
559 Josef Dai, Xuehai Pan, Ruiyang Sun, Jiaming Ji, Xinbo Xu, Mickel Liu, Yizhou Wang, and Yaodong
560 Yang. Safe rlhf: Safe reinforcement learning from human feedback. In *ICLR*, 2024.
- 561
562 Ameet Deshpande, Vishvak Murahari, Tanmay Rajpurohit, Ashwin Kalyan, and Karthik R
563 Narasimhan. Toxicity in chatgpt: Analyzing persona-assigned language models. In *EMNLP*,
564 2023.
- 565 Neil Houlsby, Andrei Giurgiu, Stanislaw Jastrzebski, Bruna Morrone, Quentin De Laroussilhe,
566 Andrea Gesmundo, Mona Attariyan, and Sylvain Gelly. Parameter-efficient transfer learning for
567 nlp. In *ICML*, 2019.
- 568
569 Chia-Yi Hsu, Yu-Lin Tsai, Chih-Hsun Lin, Pin-Yu Chen, Chia-Mu Yu, and Chun-Ying Huang. Safe
570 lora: the silver lining of reducing safety risks when fine-tuning large language models. *arXiv*
571 *preprint arXiv:2405.16833*, 2024.
- 572 Edward J Hu, Phillip Wallis, Zeyuan Allen-Zhu, Yuanzhi Li, Shean Wang, Lu Wang, Weizhu Chen,
573 et al. Lora: Low-rank adaptation of large language models. In *ICLR*, 2021.
- 574
575 Tiansheng Huang, Sihao Hu, and Ling Liu. Vaccine: Perturbation-aware alignment for large language
576 model. *arXiv preprint arXiv:2402.01109*, 2024.
- 577
578 Albert Q Jiang, Alexandre Sablayrolles, Arthur Mensch, Chris Bamford, Devendra Singh Chaplot,
579 Diego de las Casas, Florian Bressand, Gianna Lengyel, Guillaume Lample, Lucile Saulnier, et al.
580 Mistral 7b. *arXiv preprint arXiv:2310.06825*, 2023.
- 581 Dawid Jan Kopiczko, Tijmen Blankevoort, and Yuki Markus Asano. Vera: Vector-based random
582 matrix adaptation. In *ICLR*, 2024.
- 583
584 Woosuk Kwon, Zhuohan Li, Siyuan Zhuang, Ying Sheng, Lianmin Zheng, Cody Hao Yu, Joseph E.
585 Gonzalez, Hao Zhang, and Ion Stoica. Efficient memory management for large language model
586 serving with pagedattention. In *SOSP*, 2023.
- 587
588 Andrew Lee, Xiaoyan Bai, Itamar Pres, Martin Wattenberg, Jonathan K. Kummerfeld, and Rada
589 Mihalcea. A mechanistic understanding of alignment algorithms: A case study on DPO and
590 toxicity. *CoRR*, abs/2401.01967, 2024.
- 591
592 N Lee, T Ajanthan, and P Torr. Snip: Single-shot network pruning based on connection sensitivity.
593 In *ICLR*, 2019.
- Simon Lermen and Charlie Rogers-Smith. LoRA fine-tuning efficiently undoes safety training in
llama 2-chat 70b. In *ICLR Workshop*, 2024.

- 594 Brian Lester and Rami Al-Rfou Noah Constant. The power of scale for parameter-efficient prompt
595 tuning. In *EMNLP*, 2021.
- 596
- 597 Chunyuan Li, Heerad Farkhoor, Rosanne Liu, and Jason Yosinski. Measuring the intrinsic dimension
598 of objective landscapes. In *ICLR*, 2018.
- 599
- 600 Kenneth Li, Oam Patel, Fernanda B. Viégas, Hanspeter Pfister, and Martin Wattenberg. Inference-time
601 intervention: Eliciting truthful answers from a language model. In *NeurIPS*, 2023.
- 602
- 603 Kenneth Li, Oam Patel, Fernanda Viégas, Hanspeter Pfister, and Martin Wattenberg. Inference-time
604 intervention: Eliciting truthful answers from a language model. In *NeurIPS*, 2024.
- 605
- 606 Shih-Yang Liu, Chien-Yi Wang, Hongxu Yin, Pavlo Molchanov, Yu-Chiang Frank Wang, Kwang-
607 Ting Cheng, and Min-Hung Chen. Dora: Weight-decomposed low-rank adaptation. In *ICML*,
2024.
- 608
- 609 Xiaogeng Liu, Nan Xu, Muhao Chen, and Chaowei Xiao. Autodan: Generating stealthy jailbreak
610 prompts on aligned large language models. *CoRR abs/2310.04451*, 2023a.
- 611
- 612 Zhiheng Liu, Ruili Feng, Kai Zhu, Yifei Zhang, Kecheng Zheng, Yu Liu, Deli Zhao, Jingren Zhou,
613 and Yang Cao. Cones: concept neurons in diffusion models for customized generation. In *ICML*,
2023b.
- 614
- 615 AI @ Meta Llama Team. The llama 3 herd of models, 2024.
- 616
- 617 I Loshchilov. Decoupled weight decay regularization. In *ICLR*, 2019.
- 618
- 619 Sourab Mangrulkar, Sylvain Gugger, Lysandre Debut, Younes Belkada, Sayak Paul, and Benjamin
620 Bossan. Peft: State-of-the-art parameter-efficient fine-tuning methods, 2022.
- 621
- 622 Fanxu Meng, Zhaohui Wang, and Muhan Zhang. Pissa: Principal singular values and singular vectors
623 adaptation of large language models. *arXiv preprint arXiv:2404.02948*, 2024.
- 624
- 625 Jishnu Mukhoti, Yarin Gal, Philip HS Torr, and Puneet K Dokania. Fine-tuning can cripple your
626 foundation model; preserving features may be the solution. *arXiv preprint arXiv:2308.13320*,
627 2023.
- 628
- 629 OpenAI. Introducing chatgpt. <https://openai.com/blog/chatgpt>, 2022.
- 630
- 631 OpenAI. Gpt-4 technical report, 2023.
- 632
- 633 Long Ouyang, Jeffrey Wu, Xu Jiang, Diogo Almeida, Carroll L. Wainwright, Pamela Mishkin, Chong
634 Zhang, Sandhini Agarwal, Katarina Slama, Alex Ray, John Schulman, Jacob Hilton, Fraser Kelton,
635 Luke Miller, Maddie Simens, Amanda Askell, Peter Welinder, Paul F. Christiano, Jan Leike, and
636 Ryan Lowe. Training language models to follow instructions with human feedback. In *NeurIPS*,
2022.
- 637
- 638 Matthew E. Peters, Mark Neumann, Luke Zettlemoyer, and Wen-tau Yih. Dissecting contextual word
639 embeddings: Architecture and representation. In *EMNLP*, 2018.
- 640
- 641 Nicholas Pochinkov and Nandi Schoots. Dissecting language models: Machine unlearning via
642 selective pruning. *arXiv preprint arXiv:2403.01267*, 2024.
- 643
- 644 Xiangyu Qi, Yi Zeng, Tinghao Xie, Pin-Yu Chen, Ruoxi Jia, Prateek Mittal, and Peter Henderson.
645 Fine-tuning aligned language models compromises safety, even when users do not intend to! In
646 *ICLR*, 2023.
- 647
- 648 Chengwei Qin, Aston Zhang, Zhuosheng Zhang, Jiaao Chen, Michihiro Yasunaga, and Diyi Yang. Is
649 chatgpt a general-purpose natural language processing task solver? In *EMNLP*, 2023.
- 650
- 651 Rafael Rafailov, Archit Sharma, Eric Mitchell, Christopher D Manning, Stefano Ermon, and Chelsea
652 Finn. Direct preference optimization: Your language model is secretly a reward model. In *NeurIPS*,
653 2024.

- 648 Anastasia Razdaibiedina, Yuning Mao, Rui Hou, Madian Khabsa, Mike Lewis, Jimmy Ba, and Amjad
649 Almahairi. Residual prompt tuning: Improving prompt tuning with residual reparameterization. In
650 *ACL*, 2023.
- 651 Wai Man Si, Michael Backes, Jeremy Blackburn, Emiliano De Cristofaro, Gianluca Stringhini,
652 Savvas Zannettou, and Yang Zhang. Why so toxic? measuring and triggering toxic behavior in
653 open-domain chatbots. In *CCS*, 2022.
- 654 Mingjie Sun, Zhuang Liu, Anna Bair, and J Zico Kolter. A simple and effective pruning approach for
655 large language models. In *ICLR*, 2023.
- 656 Alon Talmor, Jonathan Herzig, Nicholas Lourie, and Jonathan Berant. CommonsenseQA: A question
657 answering challenge targeting commonsense knowledge. In *NAACL*, 2019.
- 658 Gemini Team, Rohan Anil, Sebastian Borgeaud, Yonghui Wu, Jean-Baptiste Alayrac, Jiahui Yu, Radu
659 Soricut, Johan Schalkwyk, Andrew M Dai, Anja Hauth, et al. Gemini: A family of highly capable
660 multimodal models. *arXiv preprint arXiv:2312.11805*, 2023.
- 661 Hugo Touvron, Thibaut Lavril, Gautier Izacard, Xavier Martinet, Marie-Anne Lachaux, Timothée
662 Lacroix, Baptiste Rozière, Naman Goyal, Eric Hambro, Faisal Azhar, et al. Llama: Open and
663 efficient foundation language models. *arXiv preprint arXiv:2302.13971*, 2023a.
- 664 Hugo Touvron, Louis Martin, Kevin Stone, Peter Albert, Amjad Almahairi, Yasmine Babaei, Nikolay
665 Bashlykov, Soumya Batra, Prajjwal Bhargava, Shrutu Bhosale, et al. Llama 2: Open foundation
666 and fine-tuned chat models. *arXiv preprint arXiv:2307.09288*, 2023b.
- 667 Pengyu Wang, Dong Zhang, Linyang Li, Chenkun Tan, Xinghao Wang, Ke Ren, Botian Jiang,
668 and Xipeng Qiu. Inferaligner: Inference-time alignment for harmlessness through cross-model
669 guidance. *arXiv preprint arXiv:2401.11206*, 2024.
- 670 Yizhong Wang, Yeganeh Kordi, Swaroop Mishra, Alisa Liu, Noah A Smith, Daniel Khashabi, and
671 Hannaneh Hajishirzi. Self-instruct: Aligning language models with self-generated instructions. In
672 *ACL*, pp. 13484–13508, 2023.
- 673 Boyi Wei, Kaixuan Huang, Yangsibo Huang, Tinghao Xie, Xiangyu Qi, Mengzhou Xia, Prateek
674 Mittal, Mengdi Wang, and Peter Henderson. Assessing the brittleness of safety alignment via
675 pruning and low-rank modifications. In *ICML*, 2024.
- 676 Zeming Wei, Yifei Wang, and Yisen Wang. Jailbreak and guard aligned language models with only
677 few in-context demonstrations. *arXiv preprint arXiv:2310.06387*, 2023.
- 678 Yueqi Xie, Jingwei Yi, Jiawei Shao, Justin Curl, Lingjuan Lyu, Qifeng Chen, Xing Xie, and Fangzhao
679 Wu. Defending chatgpt against jailbreak attack via self-reminders. *Nature Machine Intelligence*, 5
680 (12):1486–1496, 2023.
- 681 Zhangchen Xu, Fengqing Jiang, Luyao Niu, Jinyuan Jia, Bill Yuchen Lin, and Radha Poovendran.
682 Safedecoding: Defending against jailbreak attacks via safety-aware decoding. *arXiv preprint
683 arXiv:2402.08983*, 2024.
- 684 Yang Zhao, Hao Zhang, and Xiuyuan Hu. Penalizing gradient norm for efficiently improving
685 generalization in deep learning. In *ICML*, 2022.
- 686 Terry Yue Zhuo, Yujin Huang, Chunyang Chen, and Zhenchang Xing. Red teaming chatgpt via
687 jailbreaking: Bias, robustness, reliability and toxicity. *CoRR abs/2301.12867*, 2023.
- 688 Andy Zou, Long Phan, Sarah Chen, James Campbell, Phillip Guo, Richard Ren, Alexander Pan,
689 Xuwang Yin, Mantas Mazeika, Ann-Kathrin Dombrowski, et al. Representation engineering: A
690 top-down approach to ai transparency. *arXiv preprint arXiv:2310.01405*, 2023a.
- 691 Andy Zou, Zifan Wang, J. Zico Kolter, and Matt Fredrikson. Universal and transferable adversarial
692 attacks on aligned language models. *CoRR abs/2307.15043*, 2023b.
- 693
694
695
696
697
698
699
700
701